

# Spacelike and timelike form factors for $\omega \rightarrow \pi\gamma^*$ and $K^* \rightarrow K\gamma^*$ in the light-front quark model

Ho-Meoyng Choi

*Department of Physics, Teachers College, Kyungpook National University, Daegu, Korea 702-701*

(Received 21 March 2008; published 28 May 2008)

We investigate space- and timelike form factors for  $\omega \rightarrow \pi\gamma^*$  and  $K^* \rightarrow K\gamma^*$  decays using the light-front quark model constrained by the variational principle for the QCD-motivated effective Hamiltonian. The momentum dependent spacelike form factors are obtained in the  $q^+ = 0$  frame and then analytically continued to the timelike region. Our prediction for the timelike form factor  $F_{\omega\pi}(q^2)$  is in good agreement with the experimental data. We also find that the spacelike form factor  $F_{K^*K}(Q^2)$  for charged kaons encounters a zero because of the negative interference between the two currents to the quark and the antiquark.

DOI: [10.1103/PhysRevD.77.097301](https://doi.org/10.1103/PhysRevD.77.097301)

PACS numbers: 13.40.Gp, 12.39.Ki, 13.20.Eb

The one-photon radiative decays from the low-lying vector ( $V$ ) to pseudoscalar ( $P$ ) mesons, i.e. magnetic dipole  $V(1^3S_1) \rightarrow P(1^1S_0)\gamma$  transitions, have been the subject of continuous interest both theoretically and experimentally. These processes provided a valuable testing ground to understand the internal structure of hadrons and thus to pin down the best phenomenological model of hadrons. In our previous light-front quark model (LFQM) analysis [1,2] based on the QCD-motivated effective Hamiltonian, we have calculated various radiative  $V \rightarrow P\gamma$  and  $P \rightarrow V\gamma$  decay widths of light-flavored mesons ( $\pi, \rho, \omega, K, K^*, \phi, \eta, \eta'$ ) [1] and heavy-flavored ones such as ( $D, D^*, D_s, D_s^*, \eta_c, J/\psi$ ) and ( $B, B^*, B_s, B_s^*, \eta_b, Y$ ) [2] and found a good agreement with the experimental data. Especially for the recent analysis of the heavy meson sector [2], we have calculated not only the decay widths but also the momentum dependent transition form factors in both space- and timelike regions. However, our previous works on the magnetic dipole transitions of light-flavored mesons [1] presented only the decay widths without showing the momentum dependent behaviors of the form factors. Particularly interesting radiative decays of light-flavored mesons may be  $\omega \rightarrow \pi\gamma^*$  and  $K^* \rightarrow K\gamma^*$  processes since the form factor for  $\omega \rightarrow \pi\gamma^*$  has already been measured in the timelike region via the decay of  $\omega \rightarrow \pi^0\mu^+\mu^-$  [3] and  $K^* \rightarrow K\gamma^*$  decays may deserve special attention in terms of  $SU(3)$  flavor symmetry breaking.

The purpose of this paper is to calculate the space- and timelike transition form factors for selected  $\omega \rightarrow \pi\gamma^*$  and  $K^* \rightarrow K\gamma^*$  processes using our LFQM [1,2] and compare with other theoretical model predictions [4–9] as well as the available data [3]. To obtain the timelike form factor  $F_{VP}(q^2)$  for  $V \rightarrow P\gamma^*$ , we have performed the analytic continuation from the spacelike ( $q^2 < 0$ ) region to the physical timelike region [ $0 \leq q^2 \leq (M_V - M_P)^2$ ]. We find that the timelike form factor  $F_{\omega\pi}(q^2)$  obtained by analytic continuation is in good agreement with the data. We also find that the charged  $K^{*\pm} \rightarrow K^\pm\gamma^*$  transition form factor encounters a zero because of the negative interfer-

ence between the two currents to the quark and the antiquark.

In our LFQM [1,2], the momentum space light-front wave function of the ground state pseudoscalar and vector mesons is given by

$$\Psi_M^{JJ_z}(x_i, \mathbf{k}_{i\perp}, \lambda_i) = \phi_R(x_i, \mathbf{k}_{i\perp}) \mathcal{R}_{\lambda_i \lambda_z}^{JJ_z}(x_i, \mathbf{k}_{i\perp}), \quad (1)$$

where  $\phi_R(x_i, \mathbf{k}_{i\perp})$  is the radial wave function and  $\mathcal{R}_{\lambda_i \lambda_z}^{JJ_z}$  is the spin-orbit wave function obtained by the interaction independent Melosh transformation [10] from the ordinary equal-time static spin-orbit wave function assigned by the quantum numbers  $J^{PC}$ . The meson wave function in Eq. (1) is represented by the Lorentz-invariant variables,  $x_i = p_i^+/P^+$ ,  $\mathbf{k}_{i\perp} = \mathbf{p}_{i\perp} - x_i \mathbf{P}_\perp$ , and  $\lambda_i$ , where  $P$ ,  $p_i$ , and  $\lambda_i$  are the meson momentum, the momenta, and the helicities of the constituent quarks, respectively. The covariant forms of the spin-orbit wave functions for pseudoscalar and vector mesons are given in Refs. [1,2].

For the radial wave function  $\phi_R$ , we use the same Gaussian wave function for both pseudoscalar and vector mesons

$$\phi(x_i, \mathbf{k}_{i\perp}) = \frac{4\pi^{3/4}}{\beta^{3/2}} \sqrt{\frac{\partial k_z}{\partial x}} \exp(-\vec{k}^2/2\beta^2), \quad (2)$$

where  $\vec{k}^2 = \mathbf{k}_\perp^2 + k_z^2$  and the Gaussian parameter  $\beta$  is related with the size of meson. Here, the longitudinal component  $k_z$  of the three momentum is given by  $k_z = (x_1 - \frac{1}{2})M_0 + (m_2^2 - m_1^2)/2M_0$  with the invariant mass  $M_0$  defined by  $M_0^2 = (\mathbf{k}_\perp^2 + m_1^2)/x_1 + (\mathbf{k}_\perp^2 + m_2^2)/x_2$ . The Jacobian  $\partial k_z/\partial x$  of the variable transformation  $\{x, \mathbf{k}_\perp\} \rightarrow \vec{k} = (\mathbf{k}_\perp, k_z)$  is included in the radial wave function so that the wave function satisfies the following normalization

$$\int_0^1 dx \int \frac{d^2\mathbf{k}_\perp}{16\pi^3} |\phi_R(x, \mathbf{k}_{i\perp})|^2 = 1. \quad (3)$$

The key idea in our LFQM [1,2,11] for mesons is to treat  $\phi_R(x, \mathbf{k}_\perp)$  as a trial function for the variational principle to the QCD-motivated effective Hamiltonian saturating the

Fock state expansion by the constituent quark and anti-quark. The QCD-motivated effective Hamiltonian for a description of the ground state meson mass spectra is given by

$$H_{q\bar{q}} = H_0 + V_{q\bar{q}} = \sqrt{m_q^2 + \vec{k}^2} + \sqrt{m_{\bar{q}}^2 + \vec{k}^2} + V_{q\bar{q}}. \quad (4)$$

In our LFQM [1,2,11], we use the two interaction potentials  $V_{q\bar{q}}$  for the pseudoscalar and vector mesons: (1) Coulomb plus harmonic oscillator (HO), and (2) Coulomb plus linear confining potentials. In addition, the hyperfine interaction, which is essential to distinguish vector from pseudoscalar mesons, is included for both cases, viz.,

$$\begin{aligned} V_{q\bar{q}} &= V_0 + V_{\text{hyp}} \\ &= a + \mathcal{V}_{\text{conf}} - \frac{4\alpha_s}{3r} + \frac{2}{3} \frac{\mathbf{S}_q \cdot \mathbf{S}_{\bar{q}}}{m_q m_{\bar{q}}} \nabla^2 V_{\text{coul}}, \end{aligned} \quad (5)$$

where  $\mathcal{V}_{\text{conf}} = b_l r(b_h r^2)$  for the linear (HO) potential and  $\langle \mathbf{S}_q \cdot \mathbf{S}_{\bar{q}} \rangle = 1/4(-3/4)$  for the vector (pseudoscalar) meson. Our variational principle to the QCD-motivated effective Hamiltonian first evaluates the expectation value of the central Hamiltonian  $H_0 + V_0$  with a trial function  $\phi_R(x_i, \mathbf{k}_{i\perp})$  that depends on the variational parameters  $\beta$  and then varies  $\beta$  until  $\langle \phi_R | (H_0 + V_0) | \phi_R \rangle$  becomes a minimum. Once these model parameters are fixed, the mass eigenvalue of each meson is obtained by  $M_{q\bar{q}} = \langle \phi_R | (H_0 + V_{q\bar{q}}) | \phi_R \rangle$ . A more detailed procedure of determining the model parameters can be found in Refs. [1,11].

The transition form factor  $F_{VP}(q^2)$  for the radiative decay of vector meson  $V(P) \rightarrow P(P')\gamma^*(q)$  is defined as

$$\langle P(P') | J_{\text{em}}^\mu | V(P, h) \rangle = ie \epsilon^{\mu\nu\rho\sigma} \epsilon_\nu(P, h) q_\rho P_\sigma F_{VP}(q^2), \quad (6)$$

where  $q = P - P'$  is the four momentum of the virtual photon and  $\epsilon_\nu(P, h)$  is the polarization vector [2] of the vector meson with four momentum  $P$  and helicity  $h$ . The coupling constant  $g_{VP\gamma}$  for real photon ( $\gamma$ ) case is determined in the limit as  $q^2 \rightarrow 0$ , i.e.  $g_{VP\gamma} = F_{VP}(q^2 = 0)$ .

We obtain the momentum dependent transition form factor  $F_{VP}(q^2)$  using the Drell-Yan-West frame ( $q^+ = q^0 + q^3 = 0$ ) [12,13] where  $q^2 = q^+ q^- - \mathbf{q}_\perp^2 = -Q^2$ , i.e.  $Q^2 > 0$  is the spacelike momentum transfer. In this frame, the matrix element of the current can be expressed as convolution integral in terms of the light-front wave function without encountering zero-mode contributions [14] as far as the “+” component of currents  $J_{\text{em}}^\mu$  is used. To obtain the timelike form factor, we analytically continue the spacelike form factor  $F_{VP}(Q^2)$  to the timelike ( $q^2 > 0$ ) region by changing  $Q^2$  to  $-q^2$  in the form factor. Furthermore, we use the transverse ( $h = \pm 1$ ) polarization to extract the coupling constant  $g_{VP\gamma}$  since the longitudinal state of the vector meson cannot convert into a real photon.

The hadronic matrix element of the plus current,  $\mathcal{M}^+ \equiv \langle P(P') | J_{\text{em}}^+ | V(P, h = +) \rangle$  in Eq. (6) is then obtained by the

convolution formula of the initial and final state light-front wave functions:

$$\begin{aligned} \mathcal{M}^+ &= \sum_j e e_j \int_0^1 \frac{dx}{16\pi^3} \int d^2\mathbf{k}_\perp \phi_R(x, \mathbf{k}'_\perp) \phi_R(x, \mathbf{k}_\perp) \\ &\quad \times \sum_{\lambda\bar{\lambda}} \mathcal{R}_{\lambda\bar{\lambda}}^{00\dagger} \frac{\bar{u}_{\lambda'}(p'_1)}{\sqrt{p_1'^+}} \gamma^+ \frac{u_\lambda(p_1)}{\sqrt{p_1^+}} \mathcal{R}_{\lambda\bar{\lambda}}^{11}, \end{aligned} \quad (7)$$

where  $\mathbf{k}'_\perp = \mathbf{k}_\perp - x_2 \mathbf{q}_\perp$ ,  $p_1^+ = p_1'^+ = x_1 P^+$ , and  $e e_j$  is the electrical charge for  $j$ -th quark flavor. Comparing with the right-hand-side of Eq. (6), we could extract the one-loop integral  $I(m_1, m_2, q^2)$  as follows [2]

$$\begin{aligned} I(m_1, m_2, q^2) &= \int_0^1 \frac{dx}{8\pi^3} \int d^2\mathbf{k}_\perp \frac{\phi(x, \mathbf{k}'_\perp) \phi(x, \mathbf{k}_\perp)}{x_1 \tilde{M}_0 \tilde{M}'_0} \\ &\quad \times \left[ \mathcal{A} + \frac{2}{\mathcal{M}_0} \left[ \mathbf{k}_\perp^2 - \frac{(\mathbf{k}_\perp \cdot \mathbf{q}_\perp)^2}{\mathbf{q}_\perp^2} \right] \right], \end{aligned} \quad (8)$$

where  $\tilde{M}_0 = \sqrt{M_0^2 - (m_1 - m_2)^2}$  and  $\mathcal{M}_0 = M_0 + m_1 + m_2$ . The primed factors are the functions of final state momenta, e.g.  $\tilde{M}'_0 = \tilde{M}'_0(x, \mathbf{k}'_\perp)$ .

The transition form factor  $F_{VP}(q^2)$  is then obtained as

$$F_{VP}(q^2) = e_1 I(m_1, m_2, q^2) + e_2 I(m_2, m_1, q^2), \quad (9)$$

and the decay width for  $V \rightarrow P\gamma$  is given by

$$\Gamma(V \rightarrow P\gamma) = \frac{\alpha}{3} g_{VP\gamma}^2 k_\gamma^3, \quad (10)$$

where  $\alpha$  is the fine-structure constant and  $k_\gamma = (M_V^2 - M_P^2)/2M_V$  is the kinematically allowed energy of the outgoing photon.

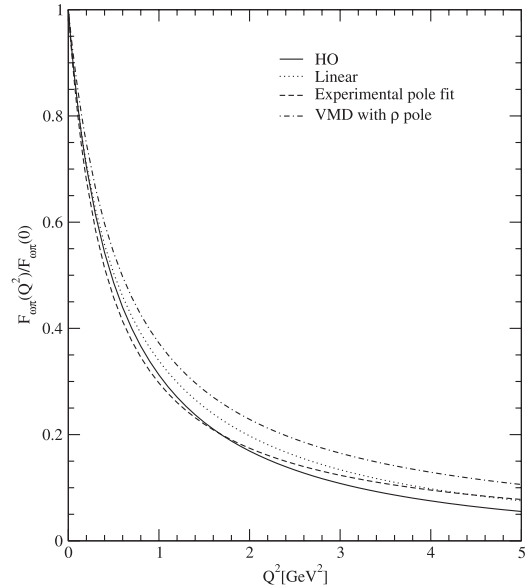


FIG. 1. The normalized transition form factor of  $\omega \rightarrow \pi^0 \gamma^*$  (or  $\rho^\pm \rightarrow \pi^\pm \gamma^*$ ) in spacelike  $Q^2$  region obtained from HO (solid line) and linear (dotted line) potential models compared with experimental pole fit (dashed line) as well as VMD model (dot-dashed line).

In our numerical calculations, we use two sets of model parameters ( $m_q = 0.22$ ,  $m_s = 0.45$ ,  $\beta_{q\bar{q}} = 0.3659$ ,  $\beta_{q\bar{s}} = 0.3886$ ) [GeV] for the linear and ( $m_q = 0.25$ ,  $m_s = 0.48$ ,  $\beta_{q\bar{q}} = 0.3194$ ,  $\beta_{q\bar{s}} = 0.3419$ ) [GeV] for HO confining potentials obtained from our variational principle [1,11], where  $q = u$  or  $d$ -quark. The isospin symmetry (i.e.  $m_u = m_d$ ) used in our LFQM implies the relation of the transition form factors  $F_{\omega\pi}(Q^2) = 3F_{\rho\pi}(Q^2)$  between  $\rho \rightarrow \pi\gamma^*$  and  $\omega \rightarrow \pi\gamma^*$  processes. In Ref. [1], we have shown that weak decay constants and electromagnetic charge radii of ( $\pi$ ,  $K$ ,  $\rho$ ,  $\omega$ ,  $K^*$ ) mesons as well as radiative decay widths for  $\rho(\omega) \rightarrow \pi\gamma$  and  $K^* \rightarrow K\gamma$  are quite comparable with the experimental data.

In Fig. 1, we show our results of the normalized transition form factor  $F_{\omega\pi}(Q^2)/F_{\omega\pi}(0)$  [or  $F_{\rho^\pm\pi^\pm}(Q^2)/F_{\rho^\pm\pi^\pm}(0)$ ] for the  $\omega \rightarrow \pi\gamma^*$  [or  $\rho^\pm \rightarrow \pi^\pm\gamma^*$ ] transition as a function of the photon momentum  $Q^2$ . The solid and dotted lines represent the results of our HO and linear potential models, respectively. The dashed and dot-dashed lines represent the results of experimental pole fit,  $F_{\omega\pi}^{\text{pole}}(Q^2) = 1/(1 + Q^2/(\Lambda_{\omega\pi}^{\text{exp}})^2)$  with  $\Lambda_{\omega\pi}^{\text{exp}} = 0.65$  GeV and vector meson dominance (VMD) model with  $\rho$  pole,  $F_{\omega\pi}^{\text{VMD}}(Q^2) = 1/(1 + Q^2/(\Lambda_{\omega\pi}^{\text{VMD}})^2)$  with  $\Lambda_{\omega\pi}^{\text{VMD}} = 0.77$  GeV, respectively. We have shown in [1] that our results for the coupling constants  $g_{\omega\pi\gamma} = 2.349[2.242]$  GeV $^{-1}$  and  $g_{\rho\pi\gamma} = 0.783[0.747]$  GeV $^{-1}$  obtained from HO [linear] model were in good agreement with the experimental data  $g_{\omega\pi\gamma}^{\text{Exp}} = (2.319 \pm 0.083)$  GeV $^{-1}$  and  $g_{\rho\pi\gamma}^{\text{Exp}} = (0.733 \pm 0.038)$  GeV $^{-1}$  [15]. As one can see from Fig. 1, the momentum dependent form factors obtained from both HO and linear models are also

quite close to  $F_{\omega\pi}^{\text{pole}}(Q^2)$  at least for small  $Q^2$  region. We also obtain the electromagnetic radius of the form factor  $F_{\omega\pi}(Q^2)$  as  $\langle r_{\omega\pi}^2 \rangle = 1.199[1.183]$  fm $^2$  for HO [linear] potential model, which can be compared with 0.897 fm $^2$  from other quark model calculation [9].

In Fig. 2, we show the timelike form factor of  $\omega \rightarrow \pi\gamma^*$  obtained from our HO model (solid line) and compare with the experimental data [3] as well as  $F_{\omega\pi}^{\text{pole}}(q^2)$  (dashed line) and  $F_{\omega\pi}^{\text{VMD}}(q^2)$  (dot-dashed line). Our result for the timelike form factor is in good agreement with the data. We should note that we only give the results below the particle production threshold ( $q^2 = 4m_q^2$ ) since the singularity for bound state production and the imaginary part will appear beyond the threshold in our model calculation.

The transition form factors for charged  $K^{*\pm} \rightarrow K^\pm\gamma^*$  and neutral  $K^{*0} \rightarrow K^0\gamma^*$  processes are quite interesting quantities as the couplings of the two currents to the quark and the antiquark differ because of the  $SU(3)$  flavor symmetry breaking. In Fig. 3, we show the normalized neutral (red online) and charged (black online)  $K^*K\gamma^*$  form factors in spacelike region obtained from our HO (solid line) and linear (dotted line) potential models, respectively. Our LFQM results are also compared with the VMD model (dot-dashed line). While the momentum dependent behaviors of  $F_{K^*0K^0}(Q^2)$  show a nearly VMD-like behavior at least for small  $Q^2$  region, those of  $F_{K^{*\pm}K^\pm}(Q^2)$  are very different from the VMD result. Especially, our  $F_{K^{*\pm}K^\pm}(Q^2)$  encounters zero at  $Q^2 \simeq 4.5$  GeV $^2$  for HO model and  $Q^2 \simeq 8$  GeV $^2$  for linear model, respectively. The authors in [6] also found form factor zero using the covariant Bethe-Salpeter (BS) model, where the zero occurs at

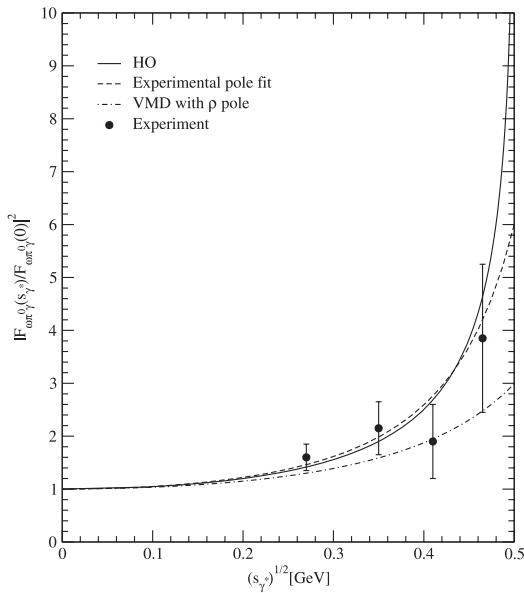


FIG. 2. Timelike  $\omega \rightarrow \pi\gamma^*$  transition form factor obtained from HO potential model (solid line) compared with experimental pole fit (dashed line) and VMD model (dot-dashed line).

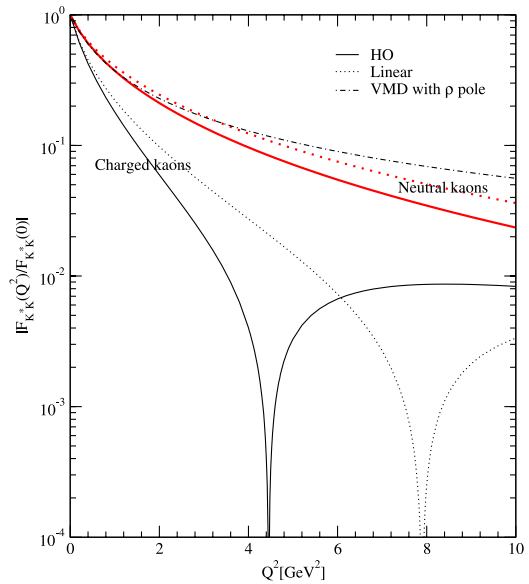


FIG. 3 (color online). The normalized neutral (red) and charged (black)  $K^*K\gamma^*$  form factors in spacelike region obtained from HO (solid line) and linear (dotted line) potential models compared with VMD model (dot-dashed line).

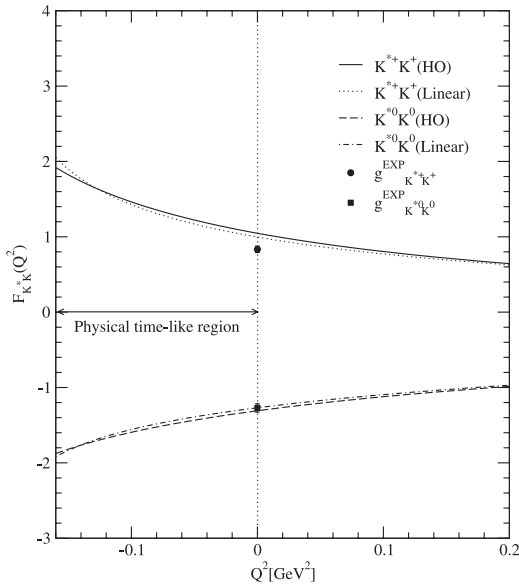


FIG. 4. The space- and timelike  $K^{*+}K^+\gamma^*$  and  $K^{*0}K^0\gamma^*$  form factors obtained from HO and linear potential models for  $-0.16 \leq Q^2 \leq 0.2$  GeV<sup>2</sup> region.

$Q^2 = 4.8$  GeV<sup>2</sup> for  $m_s/m_q = 1.8$  and moves to the right (left) as  $m_s/m_q$  decreases (increases). In our model calculation, the point of form factor zero moves to the right as  $m_s/m_q$  decreases for given  $\beta$  or as  $\beta$  increases for given  $m_s/m_q$  and vice versa. The form factor zero for  $K^{*\pm} \rightarrow K^\pm\gamma^*$  decay is mainly due to the negative interference between the two currents and depends sensitively on the ratio of the mass of the strange and nonstrange constituent quarks, i.e.  $m_s/m_q$  as well as the Gaussian  $\beta$  parameters.

In Fig. 4, we show both space- and timelike form factors of  $K^{*+} \rightarrow K^+\gamma^*$  and  $K^{*0} \rightarrow K^0\gamma^*$  transitions obtained from HO and linear potentials for  $-0.16 \leq Q^2 \leq 0.2$  GeV<sup>2</sup> region, where  $q_{\text{max}}^2 = (M_{K^*} - M_K)^2 \simeq 0.16$  GeV<sup>2</sup> and  $q^2 = 0$  correspond to a final state  $K$  meson

recoiling with zero and maximum three-momentum, respectively. The line codes are explained in the figure. While our value of the coupling constant  $g_{K^{*+}K^+\gamma} = 1.047[0.997]$  GeV<sup>-1</sup> obtained from HO [linear] model is slightly larger than the experimental data  $g_{K^{*+}K^+\gamma}^{\text{exp}} = (0.834 \pm 0.041)$  GeV<sup>-1</sup> [15],  $g_{K^{*0}K^0\gamma} = -1.309[-1.269]$  GeV<sup>-1</sup> obtained from HO [linear] is in good agreement with the data  $g_{K^{*0}K^0\gamma}^{\text{Exp}} = -(1.271 \pm 0.055)$  GeV<sup>-1</sup> [15]. The deviation of the coupling constant ratio of  $|g_{K^{*0}K^0\gamma}/g_{K^{*+}K^+\gamma}|$  from 2 implies the amount of  $SU(3)$  symmetry breaking effect [16,17]. Although our HO and linear model predictions for both neutral and charged kaon decays are somewhat different from each other in the intermediate and deep spacelike  $Q^2$  region (see Fig. 3), the two models are not much differ for the physical timelike region as well as the small  $Q^2$  region.

In this paper, we investigated the magnetic dipole  $\omega \rightarrow \pi\gamma^*$  and  $K^* \rightarrow K\gamma^*$  transitions using our LFQM constrained by the variational principle for the QCD-motivated effective Hamiltonian. The momentum dependent form factors  $F_{VP}(q^2)$  for  $V \rightarrow P\gamma^*$  decays are obtained in the  $q^+ = 0$  frame and then analytically continued to the timelike region by changing  $\mathbf{q}_\perp$  to  $i\mathbf{q}_\perp$  in the form factors. The coupling constants  $g_{VP\gamma}$  for real photon case is determined in the limit as  $q^2 \rightarrow 0$ , i.e.  $g_{VP\gamma} = F_{VP}(q^2 = 0)$ . One of the features we have investigated is the finding of the form factor zero for charged  $K^{*\pm} \rightarrow K^\pm\gamma^*$  transition, which deserves special attention from the viewpoint of experimental possibility. As a concluding remark, our model parameters obtained from the variational principle uniquely determine the above nonperturbative quantities. This approach can establish the extent of applicability of our LFQM to wider ranging hadronic phenomena.

This work was supported by Kyungpook National University Research Fund, 2007.

- 
- [1] H.-M. Choi and C.-R. Ji, Phys. Rev. D **59**, 074015 (1999).
  - [2] H.-M. Choi, Phys. Rev. D **75**, 073016 (2007).
  - [3] R.I. Dzhelyadin *et al.*, Phys. Lett. **102B**, 296 (1981).
  - [4] H. Ito and F. Gross, Phys. Rev. Lett. **71**, 2555 (1993).
  - [5] F. Cardarelli, I. L. Grach, I. M. Narodetskii, G. Salme, and S. Simula, Phys. Lett. B **359**, 1 (1995).
  - [6] C. R. Münz, J. Resag, B. C. Metsch, and H. R. Petry, Phys. Rev. C **52**, 2110 (1995).
  - [7] P. Maris and P. C. Tandy, Phys. Rev. C **65**, 045211 (2002).
  - [8] L. P. Kaptari and B. Kämpfer, Eur. Phys. J. A **31**, 233 (2007).
  - [9] J. Yu, B.-W. Xiao, and B.-Q. Ma, J. Phys. G **34**, 1845 (2007).
  - [10] H. J. Melosh, Phys. Rev. D **9**, 1095 (1974).
  - [11] H.-M. Choi and C.-R. Ji, Phys. Lett. B **460**, 461 (1999).
  - [12] S. D. Drell and T. M. Yan, Phys. Rev. Lett. **24**, 181 (1970); G. West, *ibid.* **24**, 1206 (1970).
  - [13] G. P. Lepage and S. J. Brodsky, Phys. Rev. D **22**, 2157 (1980).
  - [14] H.-M. Choi and C.-R. Ji, Phys. Rev. D **72**, 013004 (2005); **58**, 071901(R) (1998).
  - [15] W.-M. Yao *et al.* (Particle Data Group), J. Phys. G **33**, 1 (2006).
  - [16] A. Bramon and M. D. Scadron, Phys. Rev. D **40**, 3779 (1989).
  - [17] N. R. Jones and D. Liu, Phys. Rev. D **53**, 6334 (1996).